Structural Engineering and Mechanics, Vol. 22, No. 1 (2006) 107-130

DOI: http://dx.doi.org/10.12989/sem.2006.22.1.107

Numerical methods for the dynamic analysis of masonry structures

Silvia Degl'Innocenti†, Cristina Padovani‡ and Giuseppe Pasquinelli‡†

Istituto di Scienza e Tecnologie dell'Informazione "A. Faedo"
ISTI-CNR Via G. Moruzzi, 1 56124 Pisa, Italy

(Received February 25, 2005, Accepted October 17, 2005)

Abstract. The paper deals with the numerical solution of the dynamic problem of masonry structures. Masonry is modelled as a non-linear elastic material with zero tensile strength and infinite compressive strength. Due to the non-linearity of the adopted constitutive equation, the equations of the motion must be integrated directly. In particular, we apply the Newmark or the Hilber-Hughes-Taylor methods implemented in code NOSA to perform the time integration of the system of ordinary differential equations obtained from discretising the structure into finite elements. Moreover, with the aim of evaluating the effectiveness of these two methods, some dynamic problems, whose explicit solutions are known, have been solved numerically. Comparisons between the exact solutions and the corresponding approximate solutions obtained via the Newmark and Hilber-Hughes-Taylor methods show that in the cases under consideration both numerical methods yield satisfactory results.

Key words: non-linear elasticity; masonry structures; dynamic analysis; finite element method.

1. Introduction

The study of masonry structures subjected to time-dependent loads is invested with great theoretical and practical importance. The main aspects of this problem are both the choice of the constitutive equation for masonry materials, whose mechanical properties depend heavily on their constituent elements and the building techniques used, and the formulation of suitable numerical techniques for the integration of the equations of the motion.

In this paper masonry is modelled as a non-linear elastic material, with zero tensile strength and infinite compressive strength (Heyman 1966, 1982, Romano and Romano 1979, Romano and Sacco 1984, Di Pasquale 1984a,b, Como and Grimaldi 1985, Panzeca and Polizzotto 1988, Del Piero 1989, Lucchesi *et al.* 1994). This constitutive equation is able to account for some of masonry's peculiarities, in particular its inability to withstand large tensile stresses. Assumptions underlying the model are that the infinitesimal strain is the sum of an elastic part and a fracture part, and that the stress, negative semi-definite, depends linearly and isotropically on the former and is orthogonal to the latter, which is positive semi-definite. Thus, the stress is a non-linear function of the

† Technical Collaborator
‡ Research Staff, Corresponding author, E-mail: cristina.padovani@isti.cnr.it
‡† Research Staff

infinitesimal strain. This equation, known as the equation of *masonry-like* or *no-tension* materials, has been implemented in the finite element code NOSA, with the purpose of studying the static behaviour of masonry solids and modelling restoration and reinforcement operations on constructions of particular architectural interest (Lucchesi *et al.* 2000).

Regarding solution of the dynamics problem, it is necessary to directly integrate the equations of motion. In fact, due to the non-linearity of the adopted constitutive equation, the mode-superposition method is meaningless.

Instead, we perform the integration with respect to the time of the system of ordinary differential equations obtained from discretising the structure into finite elements, by implementing the Newmark (Bathe and Wilson 1976) and the Hilber-Hughes-Taylor methods (Hilber *et al.* 1977) in NOSA. Moreover, the Newton-Raphson scheme, needed to solve the non-linear algebraic system obtained at each time step, has been adapted to the dynamic case. With the aim of evaluating the effectiveness of the Newmark and Hilber-Hughes-Taylor methods, some dynamic problems whose explicit solutions are known (Casarosa *et al.* 1997, Lucchesi *et al.* 1999b, Lucchesi 2000) have been numerically solved.

A well known, specific property of the longitudinal vibrations of finite (Casarosa *et al.* 1997) and infinite (Lucchesi *et al.* 1999b) beams made of a masonry-like material is that, due to the non-linearity of the constitutive equation, shock waves arise at the interface between the zone of positive strain and that in which the strain is negative, with a consequent loss of mechanical energy and progressive decay of the solution. Comparisons between the exact solutions calculated in (Casarosa *et al.* 1997, Lucchesi *et al.* 1999b, Lucchesi 2000) and the corresponding approximate solutions obtained via the Newmark and Hilber-Hughes-Taylor methods show that in the examples considered here both numerical methods yield satisfactory results. However, these methods assume the smoothness of the velocity, while it is actually discontinuous in correspondence of the shock wave.

2. Masonry-like materials

2.1 The constitutive equation

The constitutive equation of *masonry-like* materials is based on three assumptions: infinitesimal elasticity, zero tensile strength and a normality postulate. For a more detailed treatment of this subject, refer to (Heyman 1966, 1982, Romano and Romano 1979, Romano and Sacco 1984, Di Pasquale 1984a,b, Como and Grimaldi 1985, Panzeca and Polizzotto 1988, Del Piero 1989, Lucchesi *et al.* 1994, 1995, 1996); herein, we shall limit ourselves to recalling some fundamental results.

Let $\mathcal{V}$ be a two-dimensional vector space, *Sym* the vector space of symmetric tensors on $\mathcal{V}$ equipped with the inner product $\mathbf{A} \cdot \mathbf{B} = tr(\mathbf{AB})$, $\mathbf{A}, \mathbf{B} \in Sym$, with tr the trace. We denote by Sym^+ and Sym^- the convex cones of *Sym* constituted by the positive and negative semi-definite tensors, respectively.

Let $\mathbf{T} \in Sym$ be the Cauchy stress tensor and $\mathbf{E} \in Sym$ the infinitesimal strain tensor, $\mathbf{E} = 1/2(\nabla\mathbf{u} + \nabla\mathbf{u}^T)$, where $\mathbf{u}$ is the displacement vector. We assume that $\mathbf{E}$ is the sum of an elastic part $\mathbf{E}^e$ and a fracture part $\mathbf{E}^f$

$$\mathbf{E} = \mathbf{E}^e + \mathbf{E}^f \tag{1}$$

and that $\mathbf{T}$ depends linearly and isotropically on $\mathbf{E}^e$

$$\mathbf{T} = \mathbb{C}[\mathbf{E}^e] \tag{2}$$

where

$$\mathbb{C} = \frac{E}{1+\nu}\mathbb{I} + \frac{E\nu}{(1+\nu)(1-2\nu)}\mathbf{I}\otimes\mathbf{I} \tag{3}$$

In (3) E and ν are respectively the Young' modulus and the Poisson's ratio of the material, $\mathbb{I}$ is the fourth-order identity tensor, $\mathbf{I}$ is the identity of *Sym* and $\mathbf{I}\otimes\mathbf{I}[\mathbf{A}] = tr(\mathbf{A})\mathbf{I}$ for each $\mathbf{A} \in Sym$. In particular, the fourth-order tensor $\mathbb{C}$ is symmetric and positive definite in view of the following inequalities satisfied by E and ν,

$$E > 0, \quad 0 \le \nu < \frac{1}{2} \tag{4}$$

Lastly, we assume that $\mathbf{T}$ is negative semi-definite

$$\mathbf{T} \in Sym^{-} \tag{5}$$

and that $\mathbf{E}^f$ is positive semi-definite and orthogonal to $\mathbf{T}$,

$$\mathbf{E}^f \in Sym^{+} \tag{6}$$

$$\mathbf{T}\cdot\mathbf{E}^f = 0 \tag{7}$$

From (5), (6) and (7) it follows that $\mathbf{T}$ and $\mathbf{E}^f$ are coaxial. $\mathbf{E}^f$ is called fracture strain because if it is non-null in any region of the structure, then we can expect fractures to be present in that region. If for any $\mathbf{v} \in \mathcal{V}$, $\mathbf{v}\cdot\mathbf{E}^f\mathbf{v} > 0$, $\mathbf{v}$ is not necessarily a fracture direction, in other words, $\mathbf{v}$ is not necessarily an eigenvector of $\mathbf{T}$ corresponding to the zero eigenvalue. Nonetheless, there must surely exists at least one eigenvector $\mathbf{q}$ of $\mathbf{E}^f$ (in view of the coaxiality of $\mathbf{E}^f$ and $\mathbf{T}$, $\mathbf{q}$ is also an eigenvector of $\mathbf{T}$) such that $\mathbf{q}\cdot\mathbf{E}^f\mathbf{q} > 0$ and then, in view of (7), $\mathbf{q}\cdot\mathbf{T}\mathbf{q} = 0$. Thus, if $\mathcal{F}$ is a fracture line, then every vector orthogonal to $\mathcal{F}$ is an eigenvector of $\mathbf{T}$ corresponding to the eigenvalue zero and an eigenvector of $\mathbf{E}^f$ corresponding to a positive eigenvalue.

Let $\hat{\mathbf{T}}$ denote the function that to each strain tensor $\mathbf{E}$ associates the stress $\mathbf{T}$ defined by the constitutive Eqs. (1), (2), (5), (6) and (7),

$$\mathbf{T} = \hat{\mathbf{T}}(\mathbf{E}) \tag{8}$$

Function $\hat{\mathbf{T}}$ is non-linear, Lipschitz continuous, monotone, non invertible and not differentiable everywhere in *Sym* (Del Piero 1989). The derivative $D_E\hat{\mathbf{T}}(\mathbf{E})$ of $\hat{\mathbf{T}}$ with respect to $\mathbf{E}$ has been explicitly calculated in Lucchesi *et al.* (1994, 1996); here, we shall limit ourselves to recall the expression of $D_E\hat{\mathbf{T}}(\mathbf{E})$, where it exists. In view of the application in question, we limit ourselves to consider plane stress and plane strain states. For $\mathbf{E} \in Sym$, let $e_1 \le e_2$ be its eigenvalues, $\mathbf{q}_1$, $\mathbf{q}_2$ the corresponding orthogonal unit eigenvectors and define the following tensors

$$\mathbf{O}_{11} = \mathbf{q}_1\otimes\mathbf{q}_1, \quad \mathbf{O}_{22} = \mathbf{q}_2\otimes\mathbf{q}_2, \quad \mathbf{O}_{12} = \frac{1}{\sqrt{2}}(\mathbf{q}_1\otimes\mathbf{q}_2 + \mathbf{q}_2\otimes\mathbf{q}_1) \tag{9}$$

For a plane strain the derivative $D_E\hat{\mathbf{T}}(\mathbf{E})$ of $\hat{\mathbf{T}}$ with respect to $\mathbf{E}$ is

$$D_E\hat{\mathbf{T}}(\mathbf{E}) = \frac{E}{1+\nu}\mathbb{I} + \frac{E\nu}{(1+\nu)(1-2\nu)}\mathbf{I}\otimes\mathbf{I}, \quad \text{if} \quad \mathbf{E}\in\mathcal{R}_1 \tag{10}$$

$$D_E\hat{\mathbf{T}}(\mathbf{E}) = \mathbb{O}, \quad \text{if} \quad \mathbf{E}\in\mathcal{R}_2 \tag{11}$$

$$D_E\hat{\mathbf{T}}(\mathbf{E}) = \varphi\Big(\mathbf{O}_{11}\otimes\mathbf{O}_{11} + \frac{e_1}{e_1-e_2}\mathbf{O}_{12}\otimes\mathbf{O}_{12}\Big), \quad \text{if} \quad \mathbf{E}\in\mathcal{R}_3 \tag{12}$$

where

$$\mathcal{R}_1 = \{\mathbf{E}\in Sym \,|\, \pi e_1 + (2+\pi)e_2 < 0\} \tag{13}$$

$$\mathcal{R}_2 = \{\mathbf{E}\in Sym \,|\, e_1 > 0\} \tag{14}$$

$$\mathcal{R}_3 = \{\mathbf{E}\in Sym \,|\, \pi e_1 + (2+\pi)e_2 > 0,\, e_1 < 0\} \tag{15}$$

$\pi = \dfrac{2\nu}{1-2\nu}$ and $\varphi = \dfrac{E}{1-\nu^2}$.

Although tensor $D_E\hat{\mathbf{T}}(\mathbf{E})$ does not exist on the interfaces $s_{13} = \{\mathbf{E}\in Sym|g_{13}(\mathbf{E}) = \pi e_1 + (2+\pi)e_2 = 0\}$ and $s_{23} = \{\mathbf{E}\in Sym|g_{23}(\mathbf{E}) = e_1 = 0\}$, as $\hat{\mathbf{T}}$ is Lipschitz continuous, $D_E\hat{\mathbf{T}}(\mathbf{E})$ can be replaced by the set (Curnier *et al.* 1995, Clarke 1983)

$$\partial_E\hat{\mathbf{T}}(\mathbf{E}) = \Big\{\mathbb{S}(\mathbf{E})|\mathbb{S}(\mathbf{E}) = \xi\varphi\Big(\mathbf{O}_{11}\otimes\mathbf{O}_{11} + \frac{e_1}{e_1-e_2}\mathbf{O}_{12}\otimes\mathbf{O}_{12}\Big) +$$

$$(1-\xi)\Big(\frac{E}{1+\nu}\mathbb{I} + \frac{E\nu}{(1+\nu)(1-2\nu)}\mathbf{I}\otimes\mathbf{I}\Big), \quad \xi\in[0,1]\Big\}, \quad \mathbf{E}\in s_{13} \tag{16}$$

$$\partial_E\hat{\mathbf{T}}(\mathbf{E}) = \Big\{\mathbb{S}(\mathbf{E})|\mathbb{S}(\mathbf{E}) = \xi\varphi\Big(\mathbf{O}_{11}\otimes\mathbf{O}_{11} + \frac{e_1}{e_1-e_2}\mathbf{O}_{12}\otimes\mathbf{O}_{12}\Big), \quad \xi\in[0,1]\Big\}, \quad \mathbf{E}\in s_{23} \tag{17}$$

From the relations (10)-(12) it follows that for each $\mathbf{E}\in Sym$ in which $\hat{\mathbf{T}}$ is differentiable, we have

$$D_E\hat{\mathbf{T}}(\mathbf{E})[\mathbf{E}] = \hat{\mathbf{T}}(\mathbf{E}) \tag{18}$$

$$D_E\hat{\mathbf{T}}(\mathbf{E})[\mathbf{E}^f] = \mathbf{0} \tag{19}$$

In addition, the jump $[D_E\hat{\mathbf{T}}(\mathbf{E})]$ of $D_E\hat{\mathbf{T}}(\mathbf{E})$ across the interfaces s_{13} and s_{23} satisfies the conditions given in Curnier *et al.* (1995), which express the absence of tangential discontinuity of the derivative of the stress with respect to the strain,

$$[D_E\hat{\mathbf{T}}(\mathbf{E})] = -\frac{E(1-2\nu)}{4(1-\nu^2)}\nabla g_{13}(\mathbf{E})\otimes\nabla g_{13}(\mathbf{E}), \quad \mathbf{E}\in s_{13} \tag{20}$$

$$[D_E\hat{\mathbf{T}}(\mathbf{E})] = \varphi\nabla g_{13}(\mathbf{E}) \otimes \nabla g_{13}(\mathbf{E}), \quad \mathbf{E} \in s_{23} \tag{21}$$

In particular, it holds that

$$[D_E\hat{\mathbf{T}}(\mathbf{E})][\mathbf{E}] = \mathbf{0} \tag{22}$$

for $\mathbf{E} \in s_{13}$ or $\mathbf{E} \in s_{23}$ (Padovani 2000).

Analogously, in the case of plane stress it holds that

$$D_E\hat{\mathbf{T}}(\mathbf{E}) = \frac{E}{1+\nu}\mathbb{I} + \frac{E\nu}{1-\nu^2}\mathbf{I} \otimes \mathbf{I}, \quad \mathbf{E} \in \mathcal{T}_1 \tag{23}$$

$$D_E\hat{\mathbf{T}}(\mathbf{E}) = \mathbb{O}, \quad \mathbf{E} \in \mathcal{T}_2 \tag{24}$$

$$D_E\hat{\mathbf{T}}(\mathbf{E}) = E\left(\mathbf{O}_{11} \otimes \mathbf{O}_{11} + \frac{e_1}{e_1 - e_2}\mathbf{O}_{12} \otimes \mathbf{O}_{12}\right), \quad \mathbf{E} \in \mathcal{T}_3 \tag{25}$$

where

$$\mathcal{T}_1 = \{\mathbf{E} \in Sym \,|\, \pi e_1 + 2(1+\pi)e_2 < 0\} \tag{26}$$

$$\mathcal{T}_2 = \{\mathbf{E} \in Sym \,|\, e_1 > 0\} \tag{27}$$

$$\mathcal{T}_3 = \{\mathbf{E} \in Sym \,|\, \pi e_1 + 2(1+\pi)e_2 > 0,\ e_1 < 0\} \tag{28}$$

The properties of $D_E\hat{\mathbf{T}}(\mathbf{E})$ summarized for the plane strain state also hold for the plane stress case.

The material defined by the constitutive Eqs. (1), (2), (5), (6) and (7) is hyperelastic (Del Piero 1989), and the strain-energy density coincides, within an additive constant, with the function

$$\varepsilon(\mathbf{E}) = \frac{1}{2}\hat{\mathbf{T}}(\mathbf{E}) \cdot (\mathbf{E}), \quad \mathbf{E} \in Sym \tag{29}$$

Thus, in particular, $D_E\varepsilon(\mathbf{E}) = \hat{\mathbf{T}}(\mathbf{E})$.

2.2 The mixed problem

Let $\mathcal{B}$ be a body made of a masonry-like material. We assume given on $\overline{\mathcal{B}}$ a continuous function $\rho > 0$ called density; the mass of a part $\mathcal{P}$ of $\mathcal{B}$ is then $\int_{\mathcal{P}} \rho\, dv$ (Gurtin 1972). Let $(0, t_0)$ be a fixed time interval. A motion of the body $\mathcal{B}$ is a vector field $\mathbf{u}$ on $\mathcal{B} \times (0, t_0)$. The vector $\mathbf{u}(\mathbf{x}, t)$ is the displacement vector of $\mathbf{x}$ at time t, and the fields $\dot{\mathbf{u}}$, $\ddot{\mathbf{u}}$, $\mathbf{E} = 1/2(\nabla\mathbf{u} + \nabla\mathbf{u}^T)$ and $\dot{\mathbf{E}}$ are the velocity, acceleration, strain and strain-rate.

Let us consider a body force field $\mathbf{b}$ on $\mathcal{B} \times (0, t_0)$, initial displacements $\mathbf{u}_0$ on $\mathcal{B}$, initial velocities $\mathbf{v}_0$ on $\mathcal{B}$, surface displacements $\hat{\mathbf{u}}$ on $\mathcal{S}_1 \times (0, t_0)$, surface forces $\hat{\mathbf{s}}$ on $\mathcal{S}_2 \times (0, t_0)$, where $\mathcal{S}_1$ and $\mathcal{S}_2$ are two disjoint portions of the boundary $\partial\mathcal{B}$; of $\mathcal{B}$ with $\mathcal{S}_1 \cup \mathcal{S}_2 = \partial\mathcal{B}$.

The mixed problem of the dynamics of a no-tension body consists in finding fields $\mathbf{u} : \mathcal{B} \times (0, t_0) \to \mathcal{V}$, $\mathbf{E} : \mathcal{B} \times (0, t_0) \to Sym$, $\mathbf{T} : \mathcal{B} \times (0, t_0) \to Sym$ that satisfy the congruence relation

$$\mathbf{E} = \frac{1}{2}(\nabla\mathbf{u} + \nabla\mathbf{u}^T) \tag{30}$$

the constitutive equation

$$\mathbf{T} = \hat{\mathbf{T}}(\mathbf{E}) \tag{31}$$

the equation of the motion

$$div\mathbf{T} + \mathbf{b} = \rho\ddot{\mathbf{u}} \tag{32}$$

the initial conditions

$$\mathbf{u}(\mathbf{x}, 0) = \mathbf{u}_0(\mathbf{x}), \quad \dot{\mathbf{u}}(\mathbf{x}, 0) = \mathbf{v}_0(\mathbf{x}), \quad \mathbf{x} \in \mathcal{B} \tag{33}$$

the displacement condition

$$\mathbf{u}(\mathbf{x}, t) = \hat{\mathbf{u}}(\mathbf{x}, t), \quad (\mathbf{x}, t) \in \mathcal{S}_1 \times (0, t_0) \tag{34}$$

and the traction condition

$$\mathbf{T}(\mathbf{x}, t)\mathbf{n}(\mathbf{x}) = \mathbf{s}(\mathbf{x}, t), \quad (\mathbf{x}, t) \in \mathcal{S}_2 \times (0, t_0) \tag{35}$$

where $\mathbf{n}(\mathbf{x})$ is the outward unit normal vector to $\mathcal{S}_2$ at $\mathbf{x}$. The triple $(\mathbf{u}, \mathbf{E}, \mathbf{T})$ is called solution of the mixed problem. In the framework of this formulation the uniqueness of the solution of the mixed problem in not guaranteed, even in terms of stress, which on the contrary holds for the static case (Giaquinta and Giusti 1985, Anzellotti 1985, Lucchesi *et al.* 1996). In order to avoid this inconvenience, a viscous stress $\mathbf{T}^v = \mathbb{V}[\dot{\mathbf{E}}]$ can be introduced, thanks to which the uniqueness of the displacement, strain and stress fields is recovered (Šilhavý 1997). According to the vanishing viscosity approach described in Dafermos (2000), we assume $\mathbb{V} = \alpha_1\mathbb{C}$, with α_1 as small as possible.

Setting $\mathbf{v} = \dot{\mathbf{u}}$, the Eqs. (30) and (32) can be rewritten as a first order system of balance laws,

$$\begin{cases} \dfrac{\partial E_{xx}}{\partial t} - \dfrac{\partial v_x}{\partial x} = 0 \\ \dfrac{\partial E_{yy}}{\partial t} - \dfrac{\partial v_y}{\partial y} = 0 \\ \dfrac{\partial E_{xy}}{\partial t} - \dfrac{1}{2}\left(\dfrac{\partial v_x}{\partial y} + \dfrac{\partial v_y}{\partial x}\right) = 0 \\ \rho\dfrac{\partial v_x}{\partial t} - \dfrac{\partial T_{xx}}{\partial x} - \dfrac{\partial T_{xy}}{\partial y} = b_x \\ \rho\dfrac{\partial v_y}{\partial t} - \dfrac{\partial T_{xy}}{\partial x} - \dfrac{\partial T_{yy}}{\partial y} = b_y \end{cases} \tag{36}$$

where v_x, v_y, b_x, b_y, E_{xx}, E_{yy}, E_{xy}, T_{xx}, T_{yy}, T_{xy} are the components of $\mathbf{v}$, $\mathbf{b}$, $\mathbf{E}$ and $\mathbf{T}$ with respect to a fixed orthonormal basis of $\mathcal{V}$, respectively.

Given the fourth-order tensor $D_E\hat{\mathbf{T}}(\mathbf{E})$ and the unit vector $\mathbf{m}$, let us introduce the acoustic tensor $\mathbf{A}(\mathbf{E}, \mathbf{m})$ defined by the relation (Gurtin 1972)

$$\mathbf{A}(\mathbf{E}, \mathbf{m})\mathbf{a} = \rho^{-1}D_E\hat{\mathbf{T}}(\mathbf{E})[\mathbf{a} \otimes \mathbf{m}]\mathbf{m}, \quad \text{for every } \mathbf{a} \in \mathcal{V} \tag{37}$$

We recall that system (36) is hyperbolic in the t-direction (Dafermos 2000) if for any fixed $\mathbf{U} = (E_{xx}, E_{yy}, E_{xu}, v_x, v_y)$, $(x, y, t) \in \mathcal{B} \times (0, t_0)$, and unit vector $\mathbf{g}$, the eigenvalue problem

$$[g_1 D_U \mathbf{G}_1(\mathbf{U}, x, y, t) + g_2 D_U \mathbf{G}_2(\mathbf{U}, x, y, t) - \gamma \mathbf{I}]\mathbf{R} = \mathbf{0} \tag{38}$$

with

$$\mathbf{G}_1^T = \left(-v_x,\ 0,\ -\frac{1}{2}v_y,\ -T_{xx},\ -T_{xy}\right) \tag{39}$$

and

$$\mathbf{G}_2^T = \left(0,\ -v_y,\ -\frac{1}{2}v_x,\ -T_{xy},\ -T_{yy}\right) \tag{40}$$

has five real eigenvalues $\gamma_1(\mathbf{g}, \mathbf{U}, x, y, t)$, ..., $\gamma_5(\mathbf{g}, \mathbf{U}, x, y, t)$ called characteristics speeds, and five linearly independent eigenvectors $\mathbf{R}_1(\mathbf{g}, \mathbf{U}, x, y, t)$,......, $\mathbf{R}_5(\mathbf{g}, \mathbf{U}, x, y, t)$. It can be verified that (36) is hyperbolic if for any unit vector $\mathbf{m}$ the acoustic tensor (37) is positive definite (Dafermos 2000). For a masonry-like material, there exist $\mathbf{E} \in Sym$ and unit vector $\mathbf{m}$ such that $\mathbf{A}(\mathbf{E}, \mathbf{m})$ is not positive definite. This result, proved in the Appendix, where the acoustic tensor for a plane strain state and its eigenvalues are explicitly calculated, shows that there are regions in which (36) is not hyperbolic.

Let

$$V = \frac{1}{2}\int_{\mathcal{B}} \rho \dot{\mathbf{u}}^2 dv \tag{41}$$

and

$$U = \int_{\mathcal{B}} \varepsilon dv \tag{42}$$

be the kinetic energy and the strain energy, respectively and let $T = V + U$ denote the mechanical energy. Since, in view of the constitutive equation, the inequality

$$\hat{\mathbf{T}}(\mathbf{E}) \cdot (\mathbf{E}) = \hat{\mathbf{T}}(\mathbf{E}) \cdot \mathbf{E}^e = \mathbb{C}[\mathbf{E}^e] \cdot \mathbf{E}^e \geq 0 \tag{43}$$

holds, the strain energy, analogously to the kinetic energy, is non-negative.

The classical theorem of power and energy (Gurtin 1972) which holds for linear elastic materials, states that the rate at which work is done by the surface and body forces equals the rate of change of total energy. In particular, when $\mathbf{b} = \mathbf{0}$ on $\mathcal{B}$ and $\mathbf{Tn} \cdot \dot{\mathbf{u}} = 0$ on $\partial\mathcal{B}$, then the total energy is constant. For masonry-like materials such a result is not longer true: for example, in the case of longitudinal vibrations of masonry beams (Casarosa *et al.* 1997, Lucchesi *et al.* 1999b), starting at time $t = 0$, a shock wave is generated at the interface between the unloaded and compressed regions of the beam, and consequently, the mechanical energy decreases and the solution decays (Lax 1972).

3. The numerical method

Let $\mathbf{w}$ be a vector field such that $\mathbf{w} = \mathbf{0}$ on $\mathcal{S}_1 \times (0, t_0)$, from (32) and (35) it follows that at each time t the condition of dynamic equilibrium

$$\int_{\mathcal{B}} \mathbf{T} \cdot \nabla \mathbf{w} dV + \int_{\mathcal{B}} \rho \ddot{\mathbf{u}} \cdot \mathbf{w} dV = \int_{\mathcal{B}} \mathbf{b} \cdot \mathbf{w} dV + \int_{\mathcal{S}_2} \mathbf{s} \cdot \mathbf{w} dA \tag{44}$$

must be verified. Since $\mathbf{T}$ depends non-linearly on $\mathbf{E}$, the following incremental equation

$$\int_{\mathcal{B}} \dot{\mathbf{T}} \cdot \nabla \mathbf{w} dV + \int_{\mathcal{B}} \rho \dddot{\mathbf{u}} \cdot \mathbf{w} dV = \int_{\mathcal{B}} \dot{\mathbf{b}} \cdot \mathbf{w} dV + \int_{\mathcal{S}_2} \dot{\mathbf{s}} \cdot \mathbf{w} dA \tag{45}$$

must be considered. From (45), by taking (31) into account, it follows that

$$\int_{\mathcal{B}} D_E \hat{\mathbf{T}}(\mathbf{E})[\dot{\mathbf{E}}] \cdot \nabla \mathbf{w} dV + \int_{\mathcal{B}} \rho \dddot{\mathbf{u}} \cdot \mathbf{w} dV = \int_{\mathcal{B}} \dot{\mathbf{b}} \cdot \mathbf{w} dV + \int_{\mathcal{S}_2} \dot{\mathbf{s}} \cdot \mathbf{w} dA \tag{46}$$

By applying the finite element method, and using standard techniques, the incremental Eq. (46) can be rewritten as the non-linear evolution system

$$K\dot{u} + M\dddot{u} = \dot{f} \tag{47}$$

where $\dot{u}$, $\dddot{u}$ are the velocity and the time-derivatives of the nodal accelerations. The tangent stiffness matrix K and the mass matrix M are obtained from the relations

$$c \cdot K\dot{u} = \int_{\mathcal{B}} D_E \hat{\mathbf{T}}(\mathbf{E})[\dot{\mathbf{E}}] \cdot \nabla \mathbf{w} dV \tag{48}$$

$$c \cdot M\dddot{u} = \int_{\mathcal{B}} \rho \dddot{\mathbf{u}} \cdot \mathbf{w} dV \tag{49}$$

where c is the vector of the nodal values of the field $\mathbf{w}$, and lastly,

$$c \cdot \dot{f} = \int_{\mathcal{B}} \dot{\mathbf{b}} \cdot \mathbf{w} dV + \int_{\mathcal{S}_2} \dot{\mathbf{s}} \cdot \mathbf{w} dA \tag{50}$$

Recalling that the evolution system (47) follows from the application of the finite element method to the problem (30)-(35), for which the uniqueness of the solution is not guaranteed, and bearing in mind that introduction of a viscous term allows recovery the uniqueness, in the place of system (47), we integrate the system

$$K\dot{u} + C\ddot{u} + M\dddot{u} = \dot{f} \tag{51}$$

In (51) we assume $C = \alpha_1 K^e$, where K^e is the linear elastic stiffness matrix and α_1 is a non-negative scalar chosen to be the smallest possible quantity which allows numerical solution of the system (51). In order to calculate nodal displacements, velocities and accelerations, the evolution system (51) must be integrated with respect to the time. By denoting with $f_t^{(in)}$ as the internal forces vector at time t, we assume that the equation

$$f_t^{(in)} + C\dot{u}_t + M\ddot{u}_t = f_t \tag{52}$$

holds, and the body is thus in dynamic equilibrium. Subsequently, we assign a load increment Δf defined by means of the relation

$$c \cdot \Delta f = \int_{B} (\mathbf{b}(t + \Delta t) - \mathbf{b}(t)) \cdot \mathbf{w} dV + \int_{S_2} (\mathbf{s}(t + \Delta t) - \mathbf{s}(t)) \cdot \mathbf{w} dA \tag{53}$$

and solve the linear ordinary differential equation system

$$K(u_t)\Delta u + C\Delta\dot{u} + M\Delta\ddot{u} = \Delta f \tag{54}$$

In order to solve system (54) we apply the Newmark method (Bathe and Wilson 1976). Let u_t, $\dot{u}_t$ and $\ddot{u}_t$ be, respectively, the nodal displacements, velocities and accelerations at time t. For the analogous quantities corresponding to time $t + \Delta t$ we make the following assumptions

$$\dot{u}_{t+\Delta t} = \dot{u}_t + [(1 - \delta)\ddot{u}_t + \delta\ddot{u}_{t+\Delta t}]\Delta t \tag{55}$$

$$u_{t+\Delta t} = u_t + \dot{u}_t\Delta t + \left[\left(\frac{1}{2} - \beta\right)\ddot{u}_t + \beta\ddot{u}_{t+\Delta t}\right]\Delta t^2 \tag{56}$$

with β and δ are parameters that remain to be defined. In the applications described in Section 4 we adopt the values $\beta = 1/4$ and $\delta = 1/2$ for which the Newmark method is unconditionally stable. From relations (55)-(56) we obtain the velocities and accelerations at time $t + \Delta t$ as functions of displacements $u_{t+\Delta t}$,

$$\ddot{u}_{t+\Delta t} = \frac{1}{\beta\Delta t^2}(u_{t+\Delta t} - u_t) - \frac{1}{\beta\Delta t}\dot{u}_t - \frac{1-2\beta}{2\beta}\ddot{u}_t \tag{57}$$

$$\dot{u}_{t+\Delta t} = \frac{\delta}{\beta\Delta t}(u_{t+\Delta t} - u_t) + \frac{\beta - \delta}{\beta}\dot{u}_t + \frac{2\beta - \delta}{2\beta}\ddot{u}_t\Delta t \tag{58}$$

From (57) and (58) we calculate $\Delta\dot{u}$ and $\Delta\ddot{u}$ as functions of the unknown quantity Δu,

$$\Delta\ddot{u} = \ddot{u}_{t+\Delta t} - \ddot{u}_t = \frac{1}{\beta\Delta t^2}\Delta u - \frac{1}{\beta\Delta t}\dot{u}_t - \frac{1}{2\beta}\ddot{u}_t \tag{59}$$

$$\Delta\dot{u} = \dot{u}_{t+\Delta t} - \dot{u}_t = \frac{\delta}{\beta\Delta t}\Delta u - \frac{\delta}{\beta}\dot{u}_t + \frac{2\beta - \delta}{2\beta}\ddot{u}_t\Delta t \tag{60}$$

and then, substitute the just determined relations in (54), by obtaining the system

$$W(u_t)\Delta u = \Delta f + C\left(\frac{\delta}{\beta}\dot{u}_t - \frac{2\beta - \delta}{2\beta}\ddot{u}_t\Delta t\right) + M\left(\frac{1}{\beta\Delta t}\dot{u}_t + \frac{1}{2\beta}\ddot{u}_t\right) \tag{61}$$

with

$$W(u_t) = K(u_t) + \frac{\delta}{\beta\Delta t}C + \frac{1}{\beta\Delta t^2}M \tag{62}$$

Let us now briefly describe the algorithm implemented in NOSA. Consider the following quantities related to the j-th load increment (corresponding to time $t + \Delta t$), at the i-th iteration,

$$u_{t+\Delta t}^{(i)} \tag{63}$$

is the nodal displacements vector,

$$W(u_{t+\Delta t}^{(i)}) \tag{64}$$

is the matrix of the system,

$$g_{t+\Delta t}^{(i)} \tag{65}$$

is the nodal equivalent of the assigned incremental loads, if $i = 0$; or the nodal equivalent of the residual loads, if $i \geq 1$. Let us assume that at time $t + \Delta t$ we have calculated the displacement $u_{t+\Delta t}^{(i)}$, the matrix $W(u_{t+\Delta t}^{(i)})$ and the nodal equivalent loads $g_{t+\Delta t}^{(i)}$ corresponding to the i-th iteration; in particular, $u_{t+\Delta t}^{(0)} = u_t$ and $g_{t+\Delta t}^{(0)}$ coincides with the right-hand side of (61). We now solve the system

$$W(u_{t+\Delta t}^{(i)})\Delta u_{t+\Delta t}^{(i)} = g_{t+\Delta t}^{(i)} \tag{66}$$

in order to determine the displacement

$$u_{t+\Delta t}^{(i+1)} = u_{t+\Delta t}^{(i)} + \Delta u_{t+\Delta t}^{(i)} \tag{67}$$

associated to the $i + 1$-th iteration. We then calculate the velocities

$$\dot{u}_{t+\Delta t}^{(i+1)} = \dot{u}_{t+\Delta t}^{(i)} + \Delta\dot{u}_{t+\Delta t}^{(i)} = \dot{u}_{t+\Delta t}^{(i)} + \frac{\delta}{\beta\Delta t}\Delta u_{t+\Delta t}^{(i)} - \frac{\delta}{\beta}\dot{u}_t + \frac{2\beta - \delta}{2\beta}\ddot{u}_t\Delta t \tag{68}$$

the accelerations

$$\ddot{u}_{t+\Delta t}^{(i+1)} = \ddot{u}_{t+\Delta t}^{(i)} + \Delta\ddot{u}_{t+\Delta t}^{(i)} = \ddot{u}_{t+\Delta t}^{(i)} + \frac{1}{\beta\Delta t^2}\Delta u_{t+\Delta t}^{(i)} - \frac{1}{\beta\Delta t}\dot{u}_t - \frac{1}{2\beta}\ddot{u}_t \tag{69}$$

the vector of the engineering components of stress $\sigma_{t+\Delta t}^{(i+1)}$ (in the Gauss points of the elements), the derivative of the stress with respect to strain, according to Eqs. (10)-(12) or (23)-(25), and lastly, the vector of residual loads $g_{t+\Delta t}^{(i+1)}$

$$g_{t+\Delta t}^{(i+1)} = f_t + \Delta f - \sum_{e=1}^{N}\int_{V^e} B^T\sigma_{t+\Delta t}^{(i+1)}dV^e - C\dot{u}_{t+\Delta t}^{(i+1)} - M\ddot{u}_{t+\Delta t}^{(i+1)} \tag{70}$$

In (70) matrix B connects the nodal displacements to the strains in the Gauss points of the element, and f_t is the vector of the nodal equivalent loads at time t. Lastly, we perform the convergence check; if the inequality

$$\frac{\left\|g_{t+\Delta t}^{(i+1)}\right\|}{\left\|f_t + \Delta f\right\|} \leq \xi_c \tag{71}$$

is satisfied, we go on to the next load increment $j + 1$, otherwise we repeat all operations beginning with the solution to system (66). As an alternative convergence check, we may adopt the following criterion

$$\frac{\|\delta u\|_\infty}{\|du\|_\infty} < TOL \tag{72}$$

where du is the displacement vector corresponding to the current increment, δu is the displacement vector corresponding to the current iteration, and TOL is a tolerance check parameter. In this way, the convergence is reached when the maximum displacement of the last iteration is small with respect to the maximum incremental displacement.

In 1977 Hilber, Hughes and Taylor, within the framework of linear dynamics, proposed, a method for the numerical integration of the equations of the motion which is not only unconditionally stable, but also is characterized by a numerical dissipation that can be controlled (and eventually eliminated) by a parameter that is independent of time. Such numerical dissipation damps the contribution to the solution of the modes corresponding to the higher vibration frequencies, without however influencing the modes corresponding to the lower frequencies. Subsequently, this method has also been used to solve non-linear problems (Chung and Hulbert 1993, Hulbert and Jang 1995, Geradin and Rixen 1997).

In the Hilber-Hughes-Taylor method, instead of the equation of motion (52), we consider the following modified equation

$$(1-\alpha)f_{t+\Delta t}^{(in)} + (1-\alpha)C\dot{u}_{t+\Delta t} + M\ddot{u}_{t+\Delta t} = (1-\alpha)f_{t+\Delta t} + \alpha f_t - \alpha C\dot{u}_t - \alpha f_t^{(in)} \tag{73}$$

where α is a parameter belonging to the interval [0, 1/3]. To solve Eq. (73) we use the relations (55), (56) with

$$\delta = \frac{1}{2} + \alpha, \quad \beta = \frac{1}{4}(1+\alpha)^2 \tag{74}$$

(for these values of β and δ the numerical method is unconditionally stable).

4. Examples

In this section we numerically solve the problem of the free longitudinal vibrations of a beam made of a masonry-like material subjected to different initial conditions. The corresponding exact solutions have been calculated in (Lucchesi *et al.* 1999b, Lucchesi 2000) for an infinite beam and in Casarosa *et al.* (1997) for a beam with fixed ends. The main feature of the solutions is the development of a shock wave at the interface between the cracked and compressed parts of the beam, which determines a loss of mechanical energy. As well known (Šilhavý 1997), in the presence of shock waves, the solution to the equation of the motion may be not unique. Thus, with the aim of excluding physically meaningless solutions, further conditions are required, among which the entropy condition and the Lax's E-condition.

Let us consider a beam made of a no-tension material. At time $t = 0$, a longitudinal displacement is assigned and the beam is then left to oscillate freely. The exact solution of the equation of the motion can be determined by virtue of the fact that, despite the material's non-linearity, the characteristics are straight lines. Strain and velocity are constant in certain regions of the plane (x, t), where x is the abscissa along the beam and t the time, and are discontinuous along the curves separating the different regions.

Let $u(x, t)$ be the longitudinal displacement at time t of the point having abscissa x, $u_x(x, t)$ the strain and $\varsigma = u_x/|u_x|$ its sign. For ρ the mass density and E the Young's modulus of the material, setting $\kappa = \sqrt{E/\rho}$ and $\tau = \kappa t$, let us introduce the quantity $\omega(\varsigma) = 1$ if $\varsigma = -1$, and $\omega(\varsigma) = 0$ if $\varsigma = 1$. For $u_x = 0$, $\omega(\varsigma)$ is not defined, and in this case we put $\omega(\varsigma)u_x = 0$. Hereinafter, subscripts x and τ will denote the partial derivatives with respect to x and τ. The free vibrations of the beam are governed by the partial differential equation

$$u_{\tau\tau}(x, \tau) - \omega(\varsigma)^2 u_{xx}(x, \tau) = 0 \tag{75}$$

Here we limit ourselves to considering cases in which the initial velocity is zero, thus

$$u(x, 0) = \hat{u}(x) \quad \text{and} \quad u_\tau(x) = 0, \quad -\infty < x < \infty \tag{76}$$

with $\hat{u}$ a given continuous function of x.

The solution to Eq. (75) can be calculated by using the characteristics method. In the regions where $u_x \neq 0$, there are two families of characteristic curves, $x + \tau = const$ and $x - \tau = const$, that degenerate in the unique family of vertical lines $x = const$ when $u_x > 0$. If $u_x = 0$ the characteristics are not defined. It can be verified that Eq. (75) is not genuinely non-linear and is strictly hyperbolic only if $u_x \neq 0$. We assume that the "velocity" u_τ and strain u_x have discontinuity of the first kind across a finite number of curves in the plane (x, τ). In this case, u_τ and u_x must satisfy the Rankine-Hugoniot conditions (Lax 1972)

$$s[u_x] = -[u_\tau], \quad s[u_\tau] = -[\omega^2 u_x] \tag{77}$$

where s is the "speed" of propagation of the discontinuity and the square brackets [ ] denote the jump (right minus left) across the discontinuity of the enclosed quantities.

We shall label the values of a quantity on the left and right side of the discontinuity as − and +, respectively. With the help of (77), it can be proved that if either $\varsigma^+ = \varsigma^-$, or u_x vanishes on one of the two sides, then $|s| = \omega$. Such a discontinuity is called contact discontinuity. On the contrary, if $\varsigma^+ \neq \varsigma^-$, then the discontinuity line cannot coincide with a characteristic (i.e., $|s| \neq \omega$) and it is called a shock (Lucchesi *et al.* 1999a,b). Let

$$\Psi(\tau) = \frac{1}{2}\int_{-\infty}^{+\infty} \rho\kappa^2(u_\tau^2 + \omega u_x^2)dx \tag{78}$$

be the mechanical energy of the beam, which is assumed to be bounded and differentiable for each $\tau \geq 0$. With the aim of excluding physically meaningless solutions, we require that, in the presence of discontinuities, Ψ is a non-increasing function of τ (entropy condition). Otherwise, we can require that when the characteristic beginning on either side of the discontinuity curve is continued in the direction of increasing τ, it will intersect the line of discontinuity. This is the Lax's E-condition (Lax 1972), which in our case is meaningful only when both u_x^- and u_x^+ are different from zero. The Lax's E-conditions dictates that

$$0 \geq s \geq -1, \quad \text{for} \quad s \leq 0, \quad \text{and} \quad 1 \geq s \geq 0, \quad \text{for } s \geq 0 \tag{79}$$

In particular, when $\varsigma^+ = \varsigma^- = -1$, then $|s| = 1$ and when $\varsigma^+ = \varsigma^- = 1$, then $|s| = 0$. In other words, condition (79) implies that the cracked region of the beam is in front of the shock, while the compressed one is behind it.

4.1 Longitudinal vibrations of an infinite beam with parabolic initial displacement

Let us assume that the beam is subjected to the initial conditions

$$\hat{u}(x) = \begin{cases} 0, & \text{for} \quad x \leq -\lambda \\ a\left(1 - \dfrac{x^2}{\lambda^2}\right), & \text{for} \quad -\lambda < x < \lambda \\ 0, & \text{for} \quad x \geq \lambda \end{cases} \tag{80}$$

with a and λ positive numbers, and that

$$u_\tau(x, 0) = 0 \tag{81}$$

In Lucchesi *et al.* (1999b) the explicit solution to the problem (75)-(80)-(81) has been determined by using the following property of the characteristic lines: the quantities $u_\tau + u_x$ and $u_\tau - u_x$ are constant along the characteristics $x + \tau = const.$ and $x - \tau = const.$, respectively, till they cross a shock, whereas they are not affected by crossing a contact discontinuity. The half plane $\{(x, \tau) \mid \tau > 0\}$ can be partitioned in the following regions

$$\Omega_1 = \left\{(x, \tau) \mid \tau < x < \lambda - x, \ \tau < \frac{1}{2}\lambda\right\}$$

$$\Omega_2 = \{(x, \tau) \mid -\lambda < x < \gamma_1(\tau), \ \tau < 2\lambda\}$$

$$\Omega_3 = \left\{(x, \tau) \mid \gamma_1(\tau) < x < \tau \ \text{ for } \ \tau < \frac{1}{2}\lambda, \quad \gamma_1(\tau) < x < \lambda - \tau \ \text{ for } \ \tau < 2\lambda\right\}$$

$$\Omega_4 = \{(x, \tau) \mid x > \tau + \lambda\}$$

$$\Omega_5 = \left\{(x, \tau) \mid \lambda - \tau < x < \lambda + \tau \ \text{ for } \ \tau < \frac{1}{2}\lambda, \ \ \tau < x < \lambda + \tau \ \text{ for } \ \tau > \frac{1}{2}\lambda\right\}$$

$$\Omega_6 = \left\{(x, \tau) \mid \frac{1}{2}\lambda < x < \tau, \quad \tau > \frac{1}{2}\lambda\right\}$$

$$\Omega_7 = \left\{(x, \tau) \mid \lambda - \tau < x < \frac{1}{2}\lambda \ \text{ for } \ \frac{1}{2}\lambda < \tau < 2\lambda, \ \ \gamma_2(\tau) < x < \frac{1}{2}\lambda \ \text{ for } \ \tau > 2\lambda\right\}$$

$$\Omega_8 = \{(x, \tau) \mid \lambda - \tau < x < \gamma_2(\tau), \quad \tau > 2\lambda\}$$

$$\Omega_9 = \{(x, \tau) \mid x < -\lambda, \quad \tau < \lambda - x\}$$

where $\gamma_1(\tau)$ is the straight line $x(\tau) = -\frac{1}{2}\,\tau$, and $\gamma_2(\tau)$ is the curve having equation $x(\tau) = \dfrac{\lambda}{2} - \dfrac{9\lambda^2}{2(2\tau - \lambda)}$.

γ_1 and γ_2 are shock curves because during their crossing the material goes from a state in which

$u_x > 0$ to a compressive state.

For $\varphi = \dfrac{a}{\lambda^2}$ we have

$$u_x(x,\ \tau) = -2\varphi x, \quad u_\tau(x,\ \tau) = -2\varphi\tau, \quad \text{for } (x,\ \tau) \in \Omega_1 \tag{82}$$

$$u_x(x,\ \tau) = -2\varphi x; \quad u_\tau(x,\ \tau) = 0, \quad \text{for } (x,\ \tau) \in \Omega_2 \tag{83}$$

$$u_x(x,\ \tau) = -\frac{2}{9}\varphi(5x + 4\tau), \quad u_\tau(x,\ \tau) = -\frac{2}{9}\varphi(4x + 5\tau), \quad \text{for } (x,\ \tau) \in \Omega_3 \tag{84}$$

$$u_x(x,\ \tau) = 0, \quad u_\tau(x,\ \tau) = 0, \quad \text{for } (x,\ \tau) \in \Omega_4 \tag{85}$$

$$u_x(x,\ \tau) = -\varphi(x - \tau), \quad u_\tau(x,\ \tau) = \varphi(x - \tau), \quad \text{for } (x,\ \tau) \in \Omega_5 \tag{86}$$

$$u_x(x,\ \tau) = 0, \quad u_\tau(x,\ \tau) = 0, \quad \text{for } (x,\ \tau) \in \Omega_6 \tag{87}$$

$$u_x(x,\ \tau) = \frac{4}{9}\varphi(x + \tau - \lambda), \quad u_\tau(x,\ \tau) = -\frac{2}{9}\varphi(\lambda - 2x), \quad \text{for } (x,\ \tau) \in \Omega_7 \tag{88}$$

$$u_x(x,\ \tau) = u_\tau(x,\ \tau) = -\frac{18\varphi\lambda^4}{\chi(\chi^2 + 9\lambda^2)}, \quad \text{for} \quad (x,\ \tau) \in \Omega_8 \tag{89}$$

$$u_x(x,\ \tau) = 0, \quad u_\tau(x,\ \tau) = 0, \quad \text{for} \quad (x,\ \tau) \in \Omega_9 \tag{90}$$

where $\chi = (x + \tau - \lambda) + \sqrt{(x + \tau - \lambda)^2 + 9\lambda^2}$.

The beam has been discretized with 1920 eight-node plane stress elements. Figs. 1 to 6 show the behaviour of the displacement u as function of x for different values of τ (the following parameter values have been used, $\kappa = 1666.\overline{6}$ m/s, $\rho = 1800$ kg/m^3 and $a = 10^{-4}$ m). The time integration step used in the Newmark and Hilber-Hughes-Taylor (HHT) methods is $\Delta t = 10^{-7}$ s. The red, black and the blue line respectively represent the exact solution obtained from (82)-(90), the numerical solution obtained with the Newmark method with $\alpha_1 = 10^{-7}$, and the numerical solution obtained with the Hilber-Hughes-Taylor method ($\alpha_1 = 0$, $\alpha = 0.3$), respectively.

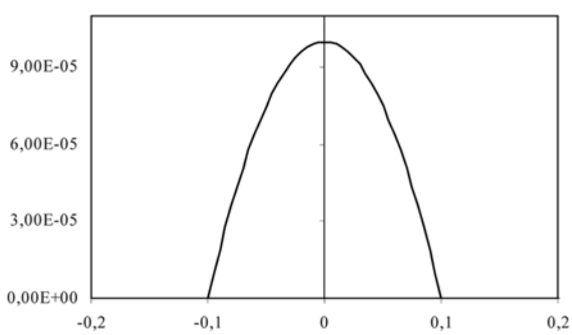

Fig. 1 Initial displacement $\hat{u}$ vs. x

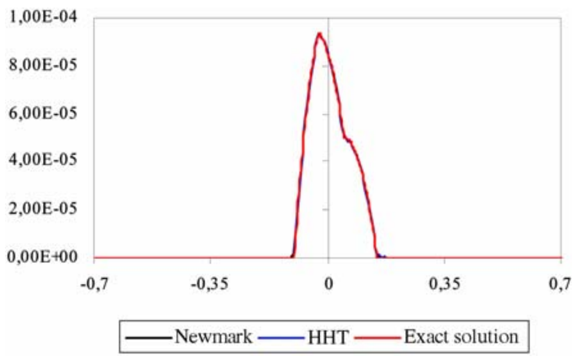

Fig. 2 Displacement u vs. x, $\tau = \dfrac{1}{2}\lambda$

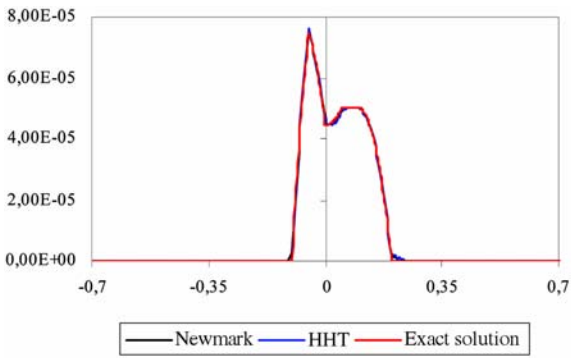

Fig. 3 Displacement u vs. x, $\tau = \lambda$

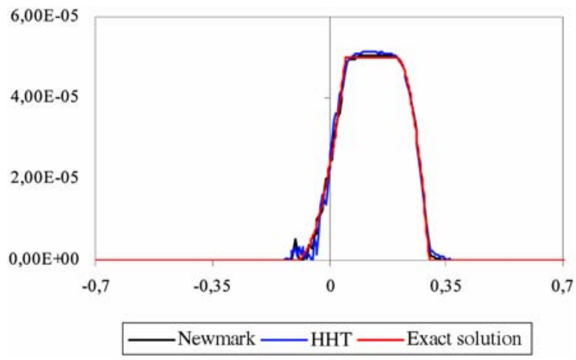

Fig. 4 Displacement u vs. x, $\tau = 2\lambda$

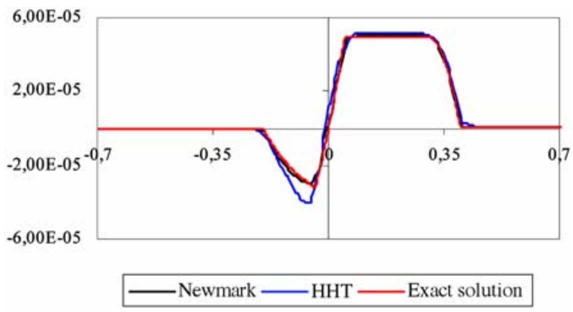

Fig. 5 Displacement u vs. x, $\tau = 3\lambda$

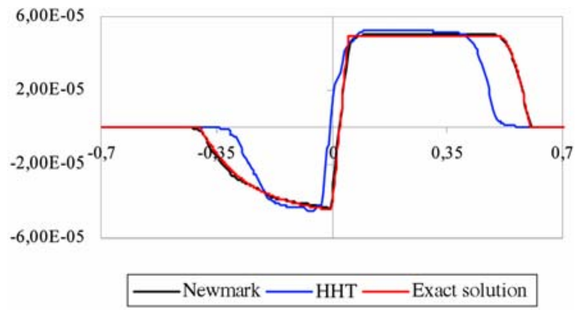

Fig. 6 Displacement u vs. x, $\tau = 5\lambda$

The behaviour of the displacement $u(\tau)$ is detailed in Lucchesi *et al.* (1999b). For $0 < \tau < \frac{1}{2}\lambda$, apart from the undisturbed regions, there are three distinct portions of the beam: the first portion has positive strain and velocity equal to zero; the second one, which is separated from the first by the shock γ_1, is compressed with negative velocity; the third one is compressed with positive velocity. For $\tau = \frac{1}{2}\lambda$ and $x = \frac{1}{2}\lambda$, when $u_x = u_\tau = 0$, two new portions of the beam arise, the former with positive strain and negative velocity, the latter with zero strain and zero velocity; a situation that continues up to the disappearance of the shock γ_1, at $\tau = 2\lambda$. For $\tau > 2\lambda$ there are four distinct portions of the beam: the first portion, where both strain and velocity are negative, spreads out, reducing the second portion, from which is separated by the shock γ_2, traveling with positive velocity.

In Lucchesi *et al.* (1999b) the expression of $\overline{\Psi}(\theta) = \dfrac{\Psi(\theta)}{\Psi(0)}$, where Ψ is the mechanical energy of the beam and $\theta = \tau/\lambda$, has been explicitly calculated

$$\overline{\Psi}(\theta) = 1 - \frac{\theta^3}{24}, \qquad \theta \in [0, 2] \tag{91}$$

$$\overline{\Psi}(\theta) = \frac{2}{3} - \frac{9}{2}\left\{\frac{1}{(2\theta-1)^3} - \frac{2}{3(2\theta-1)} + \frac{1}{9}\left[\frac{5}{3} + \frac{\pi}{2} - 2arctg\left(\frac{2\theta-1}{3}\right)\right]\right\}, \qquad \theta \geq 2 \tag{92}$$

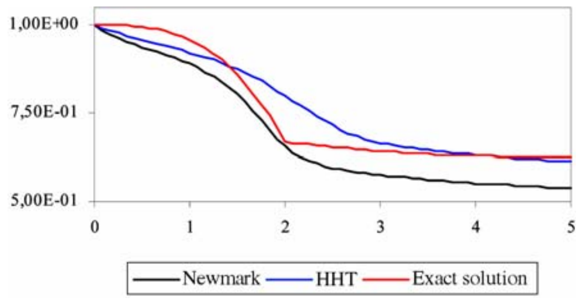

Fig. 7 Function $\overline{\Psi}$ vs. θ

In particular, $\overline{\Psi}(2) = \frac{2}{3}$ and $\lim_{\tau\to\infty} \overline{\Psi}(\theta) = \overline{\Psi}_\infty = \frac{1}{4}\left(\pi - \frac{2}{3}\right)$, thus, we have

$$\frac{\Psi(0) - \Psi(2\lambda)}{\Psi(0)} = 1 - \overline{\Psi}(2) = \frac{1}{3}, \quad 1 - \overline{\Psi}_\infty = \frac{14 - 3\pi}{12} = 0.3813 \tag{93}$$

Function $\overline{\Psi}(\theta)$ is plotted in Fig. 7; the red line represents the function (91)-(92), the black line and the blue line are the normalized energy obtained via the Newmark method ($\alpha_1 = 10^{-7}$) and the Hilber-Hughes-Taylor method ($\alpha_1 = 0$, $\alpha = 0.3$), respectively.

By looking over the diagrams, it can be seen that the best fit for the exact solution is achieved via the Newmark method, at least for $\tau \geq 2\lambda$. The curve representing the exact mechanical energy is nearly halfway between the results obtained via the two numerical schemes: Newmark fits well in the "knee" zone and HHT prevails toward the tail. On the other hand, it should be noted that Newmark method requires using an explicit damping term ($\alpha_1 > 0$) in order to obtain a converging iterative sequence. Thus, α_1 has been chosen to be as small as possible, in order to reach the convergence.

4.2 Longitudinal vibrations of an infinite beam with piecewise linear initial displacement

Now, let us assume that the beam is subjected to the initial conditions

$$\begin{cases} 0, & \text{for} \quad x \leq -\lambda \\ a\left(1 + \dfrac{x}{\lambda}\right), & \text{for} \quad -\lambda \leq x \leq 0 \\ a\left(1 - \dfrac{x}{\lambda}\right), & \text{for} \quad 0 \leq x \leq \lambda \\ 0, & \text{for} \quad x \geq \lambda \end{cases} \tag{94}$$

and (81). Based on the procedure outlined in the preceding example, with the help of the Rankine-Hugoniot conditions and the results given in Lucchesi (2000), we have calculated the displacement $u(x, \tau)$ satisfying (75), (94) and (81) for $0 \leq \tau \leq \frac{7}{2}\lambda$. Specifically, it holds that

$$u_\tau = 0, \quad u_x = 0 \tag{95}$$

in the regions $\Lambda_1 = \{(x,\ \tau)\,|\,\tau < \lambda - x,\ x < -\lambda\}$, $\Lambda_6 = \{(x,\ \tau)\,|\,\tau < -x + \lambda\}$ and $\Lambda_9 = \{(x,\ \tau)\,|\,\tau > x,\ x > \frac{1}{2}\lambda\}$;

$$u_\tau = 0, \quad u_x = \frac{a}{\lambda} \tag{96}$$

in $\Lambda_2 = \{(x,\ \tau)\,|\,\tau < -2x, x > -\lambda\}$;

$$u_\tau = -\frac{2a}{3\lambda}, \quad u_x = -\frac{a}{3\lambda} \tag{97}$$

in $\Lambda_3 = \{(x,\ \tau)\,|\,\tau > -2x,\ \tau > x,\ \tau < -x + \lambda\}$;

$$u_\tau = 0, \quad u_x = -\frac{a}{\lambda} \tag{98}$$

in $\Lambda_4 = \{(x,\ \tau)\,|\,\tau < x,\ \tau < -x + \lambda\}$;

$$u_\tau = \frac{a}{2\lambda}, \quad u_x = -\frac{a}{2\lambda} \tag{99}$$

in $\Lambda_5 = \{(x,\ \tau)\,|\,(\tau < x,\ \tau > -x + \lambda,\ \tau > x - \lambda)\}$;

$$u_\tau = -\frac{a}{3\lambda}, \quad u_x = 0 \tag{100}$$

in $\Lambda_7 = \left\{(x,\ \tau)|x < \frac{1}{2}\lambda,\ \tau > -x + \lambda,\ \tau < x + 3\lambda\right\}$ and, lastly

$$u_\tau = -\frac{a}{6\lambda}, \quad u_x = -\frac{a}{6\lambda} \tag{101}$$

in $\Lambda_8 = \{(x,\ \tau)\,|\,\tau > -x + \lambda,\ \tau > x + 3\lambda\}$.

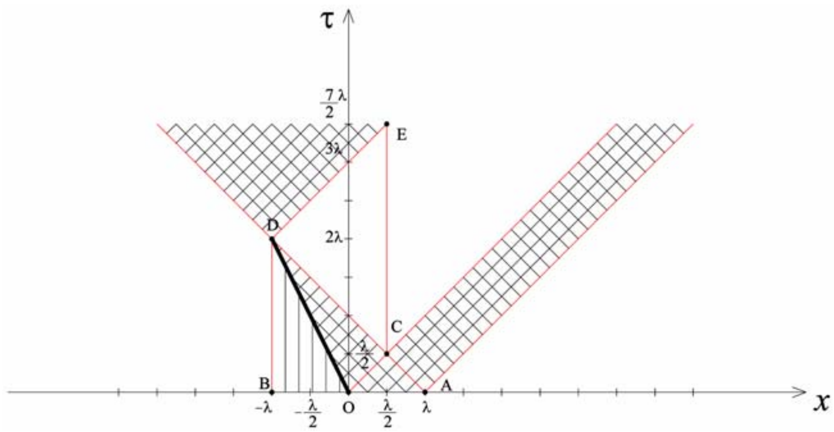

Fig. 8 Behaviour of the characteristics in the region $\{(x,\ \tau)|0 \le \tau \le \frac{7}{2}\lambda\}$

Fig. 8 shows the behaviour of the characteristics in the strip $\{(\lambda, \tau) \,|\, 0 \leq \tau \leq \frac{7}{2}\lambda\}$. Segment *OD*, with equation $x(\tau) = -\frac{1}{2}\lambda$, represents the shock. The displacement u satisfying Eq. (75), with the initial conditions (94) and (81), calculated on the basis of (95)-(101), is

$$u(x,\,\tau) \;=\; \begin{cases} 0, & \text{for} \quad x \leq -\lambda \\ \dfrac{a}{\lambda}(\lambda + x), & \text{for} \quad -\lambda \leq x \leq -\dfrac{1}{2}\tau \\ \dfrac{a}{3\lambda}(3\lambda - x - 2\tau), & \text{for} \quad -\dfrac{1}{2}\tau \leq x \leq \tau \\ \dfrac{a}{\lambda}(\lambda - x), & \text{for} \quad \tau \leq x \leq \lambda - \tau \\ \dfrac{a}{2\lambda}(\lambda - x + \tau), & \text{for} \quad \lambda - \tau \leq x \leq \lambda + \tau \\ 0, & \text{for} \quad x \geq \lambda + \tau \end{cases} \tag{102}$$

if $\tau \in \left[0, \frac{1}{2}\lambda\right]$;

$$u(x,\,\tau) \;=\; \begin{cases} 0, & \text{for} \quad x \leq -\lambda \\ \dfrac{a}{\lambda}(\lambda + x), & \text{for} \quad -\lambda \leq x \leq -\dfrac{1}{2}\tau \\ \dfrac{a}{3\lambda}(3\lambda - x - 2\tau), & \text{for} \quad -\dfrac{1}{2}\tau \leq x \leq \lambda - \tau \\ \dfrac{a}{3\lambda}(2\lambda - \tau), & \text{for} \quad \lambda - \tau \leq x < \dfrac{1}{2}\lambda \\ \dfrac{a}{2}, & \text{for} \quad \dfrac{1}{2}\lambda \leq x \leq \tau \\ \dfrac{a}{2\lambda}(\lambda - x + \tau), & \text{for} \quad \tau \leq x \leq \lambda + \tau \\ 0, & \text{for} \quad x \geq \lambda + \tau \end{cases} \tag{103}$$

if $\tau \in \left[\frac{1}{2}\lambda, 2\lambda\right]$;

$$u(x,\,\tau) \;=\; \begin{cases} 0, & \text{for} \quad x \leq \lambda - \tau \\ \dfrac{a}{6\lambda}(\lambda - x - \tau), & \text{for} \quad \lambda - \tau \leq x \leq \tau - 3\lambda \\ \dfrac{a}{3\lambda}(2\lambda - \tau), & \text{for} \quad \tau - 3\lambda \leq x < \dfrac{1}{2}\lambda \\ \dfrac{a}{2}, & \text{for} \quad \dfrac{1}{2}\lambda \leq x \leq \tau \\ \dfrac{a}{2\lambda}(\lambda - x + \tau), & \text{for} \quad \tau \leq x \leq \tau + \lambda \\ 0, & \text{for} \quad x \geq \tau + \lambda \end{cases} \tag{104}$$

if $\tau \in \left[2\lambda, \frac{7}{2}\lambda\right]$.

The discretization of the beam and the parameters κ, ρ and a are the same of the preceding subsection. Figs. 9 to 14 show the displacement u as function of x for different values of τ : the red, black and the blue lines respectively represent the exact solution, the Newmark solution ($\alpha_1 = 10^{-7}$) and the HHT solution ($\alpha_1 = 0$, $\alpha = 0.3$).

For $0 < \tau < \frac{1}{2}\lambda$, apart from the undisturbed regions, there are three distinct portions of the beam: the first portion has $u_x > 0$ and $u_\tau = 0$, the second, which is separated from the first by the shock

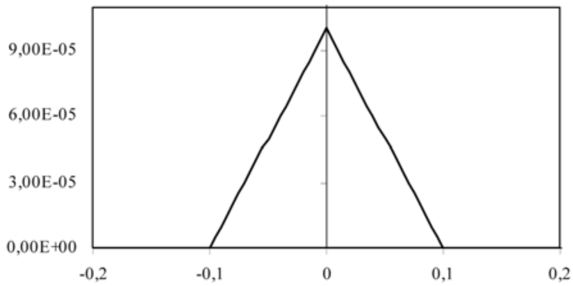

Fig. 9 Initial displacement $\hat{u}$ vs. x

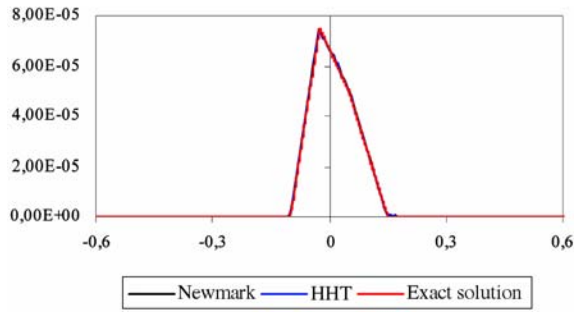

Fig. 10 Displacement u vs. x, $\tau = \frac{1}{2}\lambda$

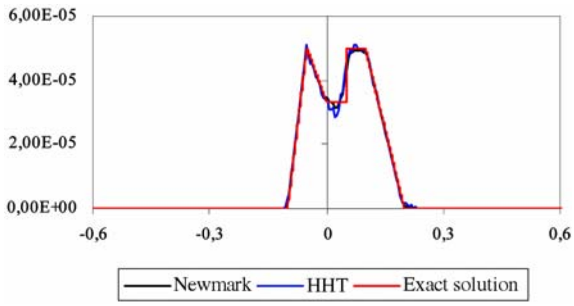

Fig. 11 Displacement u vs. x, $\tau = \lambda$

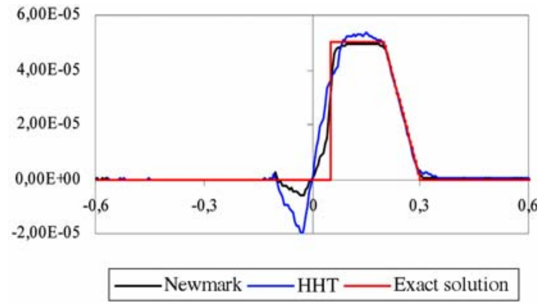

Fig. 12 Displacement u vs. x, $\tau = 2\lambda$

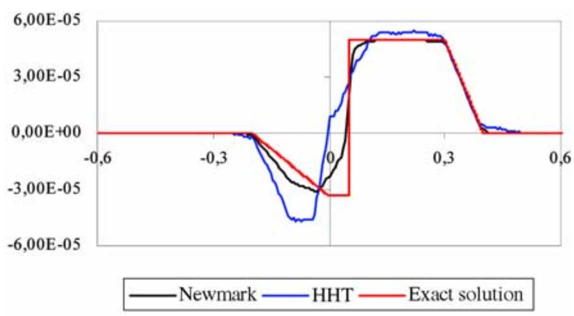

Fig. 13 Displacement u vs. x, $\tau = 3\lambda$

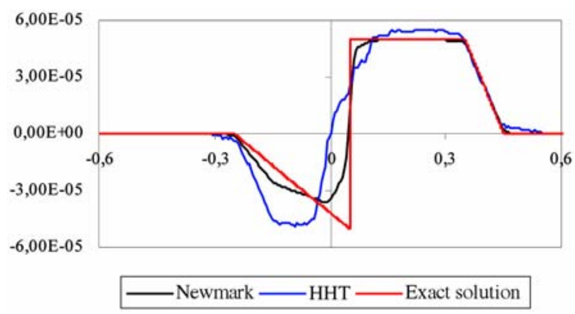

Fig. 14 Displacement u vs. x, $\tau = \frac{7}{2}\lambda$

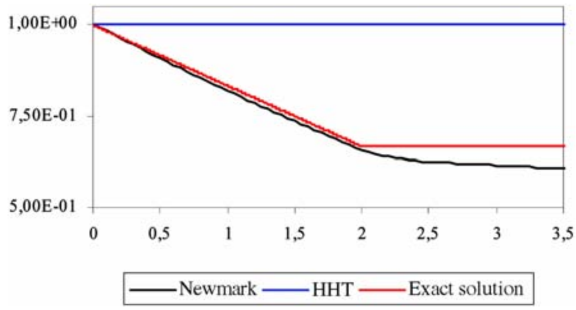

Fig. 15 Function $\overline{\Psi}$ vs. θ

OD, is compressed with $u_\tau \geq 0$; while the third is compressed with $u_\tau > 0$. For $\tau = \frac{1}{2}\lambda$ and $x = \frac{1}{2}\lambda$, two new portions arise on the beam, the former with $u_\tau < 0$ and $u_x = 0$, the latter with $u_x = u_\tau = 0$. For $\tau > \frac{1}{2}\lambda$, displacement $u(x, \tau)$ has a discontinuity of the first kind in $x = \frac{1}{2}\lambda$. The interval $\frac{1}{2}\lambda < \tau < 2\lambda$ is characterised by the fact that the compressive front in Λ_5 travels rightward causing expansion of the undisturbed region Λ_9. On the contrary, the unstrained region Λ_7 travels leftward, reducing the compressed region Λ_3, a situation that continues up to the disappearance of the shock OD at $\tau = 2\lambda$. For $2\lambda < \tau < \frac{7}{2}\lambda$ there are four distinct portions of the beam: the first portion, characterised by $u_\tau < 0$ and $u_x < 0$, spreads out, reducing the second portion, characterised by $u_\tau < 0$ and $u_x = 0$. In particular, for $\tau = \frac{7}{2}\lambda$ this portion reduces to a point, as shown in Fig. 14. The third portion, where $u_x = u_\tau = 0$, spreads out rightward, due to the fact that the fourth compressed portion travels with positive velocity.

The mechanical energy is

$$\Psi(\tau) = \begin{cases} \dfrac{\rho\kappa^2}{12}\left(\dfrac{a}{\lambda}\right)^2(6\lambda - \tau), & \text{for} \quad 0 \leq \tau \leq 2\lambda \\ \dfrac{\rho\kappa^2}{3}\dfrac{a^2}{\lambda}, & \text{for} \quad \tau \geq 2\lambda \end{cases} \tag{105}$$

Function $\overline{\Psi}(\theta)$, with $\theta = \tau/\lambda$ is plotted in Fig. 15; the red line represents the suitably normalized function (105), the black and blue lines are the normalized energy obtained via the Newark and HHT method, respectively.

The observations advanced in the preceding example hold in this case as well. The presence of a discontinuity in the displacement at $x = \frac{1}{2}\lambda$ for $\tau > \frac{1}{2}\lambda$ explains the worse fit achieved by both methods, although Newmark's results are still better, particularly regarding the mechanical energy.

4.3 Longitudinal vibrations of a beam with fixed ends

Let us consider a finite beam with length l. We are now considering the boundary conditions

$$u(0, \tau) = u(l, \tau) = 0, \quad \tau \geq 0 \tag{106}$$

and choose the initial condition

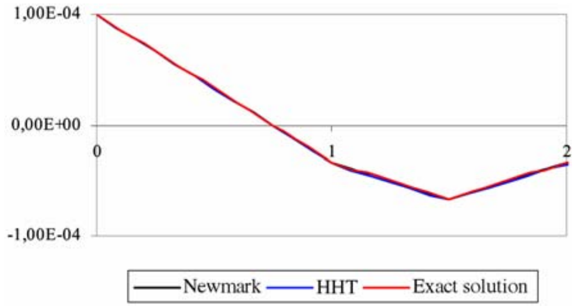

Fig. 16 $u(0.5, \tau)$ vs. $\tau \in [0, 2]$

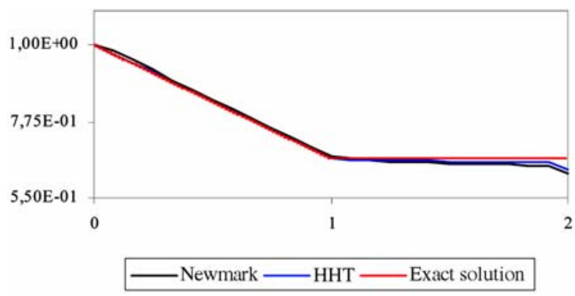

Fig. 17 Function $\overline{\Phi}(\tau)$ vs. $\tau \in [0, 2]$

$$\hat{u}(x) = \begin{cases} 2ax, & 0 \le x \le \dfrac{l}{2} \\ 2a(l-x), & \dfrac{l}{2} \le x \le l \end{cases} \tag{107}$$

It is possible to prove that (Casarosa *et al.* 1997) the displacement of the midpoint is

$$u(0.5, \tau) = \begin{cases} \dfrac{a}{3}(3-4\tau), & \tau \in [0, 1] \\ \dfrac{a}{3}(1-2\tau), & \tau \in [1, 1.5] \\ \dfrac{a}{3}(2\tau-5), & \tau \in [1.5, 2] \end{cases} \tag{108}$$

and that the mechanical energy of the beam is

$$\Phi(\tau) = \frac{1}{2}\int_0^l \rho\kappa^2 (u_\tau^2 + \omega u_x^2)dx \tag{109}$$

The beam has been discretised with 640 eight-node plane stress elements, with $l = 1$ m, $\kappa = 1666.\overline{6}$ m/s, $\rho = 1800$ kg/m^3 and $a = 10^{-4}$ m. Fig. 16 shows the behaviour of $u(0.5, \tau)$ for $\tau \in [0, 2]$ and Fig. 17 the plot of the function $\overline{\Phi}(\tau) = \Phi(\tau)/\Phi(0)$.

The red line represents the exact solution (108) and (109), the black and blue lines are the numerical solutions obtained by using the Newmark method with $\alpha_1 = 10^{-7}$, and the Hilber-Hughes-Taylor method with $\alpha_1 = 0$, $\alpha = 0.3$, respectively.

Fig. 17 indicates that a loss of mechanical energy occurs due to the formation of two shock waves (Casarosa *et al.* 1997). This phenomenon causes a progressive decay of the solution, as shown in Fig. 16.

5. Conclusions

In order to integrate with respect to the time the system of ordinary differential equations obtained by discretising the structure into finite elements, the Newmark and Hilber-Hughes-Taylor methods have been implemented in NOSA. With the aim of evaluating the effectiveness of the Newmark and Hilber-Hughes-Taylor methods, some dynamic problems whose exact solution is known (Lucchesi *et al.* 1999b, Lucchesi 2000, Casarosa *et al.* 1997), have been solved numerically.

Many trials were performed by varying the parameters α_1, α and Δt. As far as the Hilber-Hughes-Taylor method is concerned, we have verified that the choice of $\alpha_1 = 0$, $\alpha = 0.3$ (in view of (74), we have $\delta = 0.8$, $\beta = 0.4225$) yields the best results, in the sense that the displacement calculated with these values is the closest to the exact displacement. It should be noted that even in the absence of damping terms ($\alpha_1 = 0$), for $\alpha \neq 0$ a term depending on the velocity is introduced into Eq. (73); thus, the Hilber-Hughes-Taylor method presents a numerical damping. We have verified that the convergence to the solution is not guaranteed by using the Newmark method with $\alpha_1 = 0$, and that the choice $\alpha_1 = 10^{-7}$ with $\delta = 0.5$, $\beta = 0.25$ provides a good algorithm of integration. In addition, the Newmark method with $\alpha_1 = 0$ and $\delta = 0.8$, $\beta = 0.4225$ (the same values used in the HHT method) yields the same results as the Hilber-Hughes-Taylor method with $\alpha = 0.3$. Lastly, for values of Δt less than 10^{-7} s neither method provides results better than those obtained with $\Delta t = 10^{-7}$ s.

Comparison of the exact solutions with the corresponding approximations obtained via the Newmark and Hilber-Hughes-Taylor methods shows that in the examples considered here, both numerical methods provide satisfactory results, although they assume the velocity to be smooth, while in fact it is discontinuous in correspondence of the shock wave. In the cases addresses herein, the numerical solution calculated via the Newmark method provides a very good fit to the exact solution.

References

Anzellotti, G. (1985), "A class of non-coercive functionals and masonry-like materials", *Ann. Inst. Henri Poincaré*, **2**, 261-307.

Bathe, J.K.J. and Wilson, W.E.L. (1976), *Numerical Methods in Finite Element Analysis*, Prentice-Hall, Inc., Englewood Cliffs, New Jersey.

Casarosa, C., Lucchesi, M., Padovani, C., Pagni, A. and Pasquinelli, G. (1997), "Longitudinal vibrations of masonry beams", *Proc. of the Fourth Int. Symposium on Computer Methods in Structural Masonry*, 3-5 September 1997, Florence, Italy.

Chung, J. and Hulbert, G.M. (1993), "A time integration algorithm for structural dynamics with improved numerical dissipation: the generalized-α method", *J. Appl. Mech.*, **60**, 371-375, June.

Clarke, F.H. (1983), *Optimization and Nonsmooth Analysis*, John Wiley & Sons.

Clough, R.W. and Penzien, J. (1975), *Dynamics of Structures*, McGraw-Hill.

Como, M. and Grimaldi, A. (1985), "A unilateral model for the limit analysis of masonry walls", In *Unilateral Problems in Structural Analysis*, G. Del Piero and F. Maceri Eds., Springer.

Curnier, A., He, Qi-Chang and Zysset, P. (1995), "Conewise linear elastic materials", *J. of Elasticity*, **37**, 1-38.

Dafermos, C.M. (2000), *Hyperbolic Conservation Laws in Continuum Physics,* Springer-Verlag Berlin Heidelberg.

Del Piero, G. (1989), "Constitutive equation and compatibility of the external loads for linear elastic masonry-like materials", *Meccanica,* **24**, 150-162.

Di Pasquale, S. (1984a), "Questioni concernenti la meccanica dei mezzi non reagenti a trazione", *Atti VII Congresso Nazionale AIMETA*, Trieste.

Di Pasquale, S. (1984b), "Statica dei solidi murari: teoria ed esperienze", Internal Report, Dipartimento di Costruzioni, Università di Firenze.

Giaquinta, M. and Giusti, E. (1985), "Researches on the equilibrium of masonry structures", *Arch. Rational Mech. Analysis*, **8**, 359-392.
Gurtin, M.E. (1972), *The Linear Theory of Elasticity*, Encyclopedia of Physics **VIa/2** Mechanics of Solids II 1-294.
Géradin, M. and Rixen, D. (1997), *Mechanical Vibrations. Theory and Application to Structural Dynamics*, 2nd edition John Wiley & Sons Ltd.
Heyman, J. (1966), "The stone skeleton", *Int. J. Solids Struct.*, **2**, 249-279.
Heyman, J. (1982), *The Masonry Arch*, J. Wiley & Sons.
Hilber, H.M., Hughes, T.J.R. and Taylor, L.R. (1977), "Improved numerical dissipation for time integration algorithms in structural dynamics", *Earthq. Eng. Struct. Dyn.*, **5**, 283-292.
Hulbert, G.M. and Jang, I. (1995), "Automatic time step control algorithms for structural dynamics", *Comput. Meth. Appl. Mech. Eng.*, **126**, 155-178.
Lax, P.D. (1972), *Hyperbolic Systems of Conservations Laws and the Mathematical Theory of Shock Waves*, Society for Industrial and Applied Mathematics, Philadelphia.
Lucchesi, M. (2000), Private communication.
Lucchesi, M., Padovani, C. and Pagni, A. (1994), "A numerical method for solving equilibrium problems of masonry-like solids", *Meccanica,* **24**, 175-193.
Lucchesi, M., Padovani, C. and Pasquinelli, G. (1995), "On the numerical solution of equilibrium problems for elastic solids with bounded tensile strength", *Comput. Methods Appl. Mech. Engrg.*, **127**, 37-56.
Lucchesi, M., Padovani, C. and Zani, N. (1996), "Masonry-like materials with bounded compressive strength", *Int. J. Solids Struct.,* **33**, 1961-1994.
Lucchesi, M., Padovani, C., Pagni, A. and Pasquinelli, G. (1999a), "The entropy condition and Lax's E-condition for longitudianl oscillations of bimodular rods", *Proc. of PACAM VI, Sixth Pan-Americam Congress of Applied Mechanics and VIII Int. Conf. on Dynamic Problems in Mechanics*, Rio de Janeiro, 4-8 January, 1389-1392.
Lucchesi, M., Padovani, C., Pagni, A., Pasquinelli, G. and Zani N. (1999b), "Sulla propagazione delle onde longitudinali in travi non resistenti a trazione", *Atti del XIV Congresso dell'Associazione Italiana di Meccanica Teorica e Applicata*, Como 6-9 October.
Lucchesi, M., Padovani, C., Pagni, A., Pasquinelli, G. and Zani, N. (2000), "COMES-NOSA A finite element code for non-linear structural analysis", Report CNUCE-B4-2000-003.
Padovani, C. (2000), "On a class of non-linear elastic materials", *Int. J. Solids Struct.*, **37**, 7787-7807.
Panzeca, T. and Polizzotto, C. (1988), "Constitutive equations for no-tension materials", *Meccanica,* **23**, 88-93.
Romano, G. and Romano, M. (1979), "Sulla soluzione di rpoblemi strutturali in presenza di legani costitutivi unilaterali", *Rend. Acc. Naz. Lincei*, Classe di Scienze Fisiche Matematiche e Naturali, Serie VIII, **LXVII**.
Romano, G. and Sacco, E. (1984), "Sul calcolo di strutture non reagenti a trazione", *Atti VII Congresso Nazionale AIMETA*, Trieste.
Šilhavý, M. (1997), Private Communication.
Šilhavý, M. (1997), *The Mechanics and Thermodynamics of Continuous Media.* Springer Verlag, Berlin.

Appendix

Here we calculate the acoustic tensor (37) for a plane strain state. From (10), (11) and (12), we obtain

$$\mathbf{A}(\mathbf{E},\mathbf{m}) = \frac{E(1-\nu)}{\rho(1+\nu)(1-2\nu)}\mathbf{m}\otimes\mathbf{m} + \frac{E}{2\rho(1+\nu)}(\mathbf{I}-\mathbf{m}\otimes\mathbf{m}), \quad \mathbf{E}\in\mathcal{R}_1 \tag{110}$$

$$\mathbf{A}(\mathbf{E},\mathbf{m}) = \mathbf{0}, \quad \mathbf{E}\in\mathcal{R}_2 \tag{111}$$

$$\mathbf{A}(\mathbf{E},\mathbf{m}) = \frac{\varphi}{\rho}\left\{\left[(\mathbf{q}_1\cdot\mathbf{m})^2 + \frac{e_1}{2(e_1-e_2)}(\mathbf{q}_2\cdot\mathbf{m})^2\right]\mathbf{O}_1 + \frac{e_1}{2(e_1-e_2)}\mathbf{O}_2 + \frac{e_1}{\sqrt{2}(e_1-e_2)}(\mathbf{q}_1\cdot\mathbf{m})(\mathbf{q}_2\cdot\mathbf{m})\mathbf{O}_3\right\}$$

$$\mathbf{E}\in\mathcal{R}_3 \tag{112}$$

If $\mathbf{E} \in \mathcal{R}_1$, $\mathbf{A}(\mathbf{E}, \mathbf{m})$ has two positive eigenvalues

$$\eta_1 = \frac{\mu}{\rho}, \quad \eta_2 = \frac{E(1-\nu)}{\rho(1+\nu)(1-2\nu)} \tag{113}$$

then, system (36) is hyperbolic. If $\mathbf{E} \in \mathcal{R}_2$, $\mathbf{A}(\mathbf{E}, \mathbf{m})$ has two null eigenvalues. Lastly, if $\mathbf{E} \in \mathcal{R}_3$, the eigenvalues of $\mathbf{A}(\mathbf{E}, \mathbf{q}_2)$ are

$$\eta_1 = 0, \quad \eta_2 = \frac{\varphi}{\rho}\frac{e_1}{2(e_1 - e_2)} > 0 \tag{114}$$

and $\mathbf{A}(\mathbf{E}, \mathbf{m})$ has two distinct positive eigenvalues for $\mathbf{m} \neq \mathbf{q}_2$,

$$\eta_1 = \frac{\varphi}{2\rho(e_1 - e_2)}\left\{e_1 + 2(e_1 - e_2)(\mathbf{q}_1 \cdot \mathbf{m})^2 + \sqrt{4e_1^2(\mathbf{q}_1 \cdot \mathbf{m})^2(\mathbf{q}_2 \cdot \mathbf{m})^2 + [e_1 - 2e_2(\mathbf{q}_1 \cdot \mathbf{m})^2]^2}\right\} \tag{115}$$

$$\eta_2 = \frac{\varphi}{2\rho(e_1 - e_2)}\left\{e_1 + 2(e_1 - e_2)(\mathbf{q}_1 \cdot \mathbf{m})^2 - \sqrt{4e_1^2(\mathbf{q}_1 \cdot \mathbf{m})^2(\mathbf{q}_2 \cdot \mathbf{m})^2 + [e_1 - 2e_2(\mathbf{q}_1 \cdot \mathbf{m})^2]^2}\right\} \tag{116}$$

with $\eta_1 < \eta_2$.